symmetry

MDPI

Article

Behavior of Floquet Topological Quantum States in Optically Driven Semiconductors

Andreas Lubatsch [1,†] and Regine Frank [2,3,*,†]

1 University of Applied Sciences Nürnberg Georg Simon Ohm, Keßlerplatz 12, 90489 Nürnberg, Germany; lubatsch@th.physik.uni-bonn.de
2 Bell Labs, 600 Mountain Avenue, Murray Hill, NJ 07974-0636, USA
3 Serin Physics Laboratory, Department of Physics and Astronomy, Rutgers University, 136 Frelinghuysen Road, Piscataway, NJ 08854-8019, USA
* Correspondence: regine.frank@rutgers.edu or regine.frank@googlemail.com
† These authors contributed equally to this work.

Received: 22 July 2019; Accepted: 18 September 2019; Published: 4 October 2019

Abstract: Spatially uniform optical excitations can induce Floquet topological band structures within insulators which can develop similar or equal characteristics as are known from three-dimensional topological insulators. We derive in this article theoretically the development of Floquet topological quantum states for electromagnetically driven semiconductor bulk matter and we present results for the lifetime of these states and their occupation in the non-equilibrium. The direct physical impact of the mathematical precision of the Floquet-Keldysh theory is evident when we solve the driven system of a generalized Hubbard model with our framework of dynamical mean field theory (DMFT) in the non-equilibrium for a case of ZnO. The physical consequences of the topological non-equilibrium effects in our results for correlated systems are explained with their impact on optoelectronic applications.

Keywords: topological excitations; Floquet; dynamical mean field theory; non-equilibrium; stark-effect; semiconductors

PACS: 71.10.-w theories and models of many-electron systems; 42.50.Hz strong-field excitation of optical transitions in quantum systems; multi-photon processes; dynamic Stark shift; 74.40+ Fluctuations; 03.75.Lm Tunneling, Josephson effect, Bose-Einstein condensates in periodic potentials, solitons, vortices, and topological excitations; 72.20.Ht high-field and nonlinear effects; 89.75.-k complex systems

1. Introduction

Topological phases of matter [1–3] have captured our fascination over the past decades, revealing properties in the sense of robust edge modes and exotic non-Abelian excitations [4,5]. Potential applications of periodically driven quantum systems [6] are conceivable in the subjects of semiconductor spintronics [7] up to topological quantum computation [8] as well as topological lasers [9,10] in optics and random lasers [11]. Already topological insulators in solid-state devices such as HgTe/CdTe quantum wells [12,13], as well as topological Dirac insulators such as Bi_2Te_3 and Bi_2Sn_3 [14–16] were groundbreaking discoveries in the search for the unique properties of topological phases and their technological applications.

In non-equilibrium systems, it has been shown that time-periodic perturbations can induce topological properties in conventional insulators [17–20] which are trivial in equilibrium otherwise. Floquet topological insulators include a very broad range of physical solid state and atomic realizations, driven at resonance or off-resonance. These systems can display metallic conduction, which is enabled

by quasi-stationary states at the edges [17,21,22]. Their band structure may have the form of a Dirac cone in three-dimensional systems [23,24], and Floquet Majorana fermions [25] have been conceptionally developed. Graphene and Floquet fractional Chern insulators have been recently investigated [26–28].

In this article, we show that Floquet topological quantum states can evolve in correlated electronic systems of driven semi-conductors in the non-equilibrium. We investigate *ZnO* bulk matter in the centrosymmetric, cubic rocksalt configuration, see Figure 1. The non-equilibrium is in this sense defined by the intense external electromagnetic driving field, which induces topologically dressed electronic states and the evolution of dynamical gaps, see Figure 2. These procedures are expected to be observable in pump-probe experiments on time scales below the thermalization time. We show that the expansion into Floquet modes [29], see Figure 3, is leading to results of direct physical impact in the sense of modeling the coupling of a classical electromagnetic external driving field to the correlated quantum many body system. Our results derived by Dynamical Mean Field Theory (DMFT) in the non-equilibrium provide novel insights in topologically induced phase transitions of driven otherwise conventional three-dimensional semiconductor bulk matter and insulators.

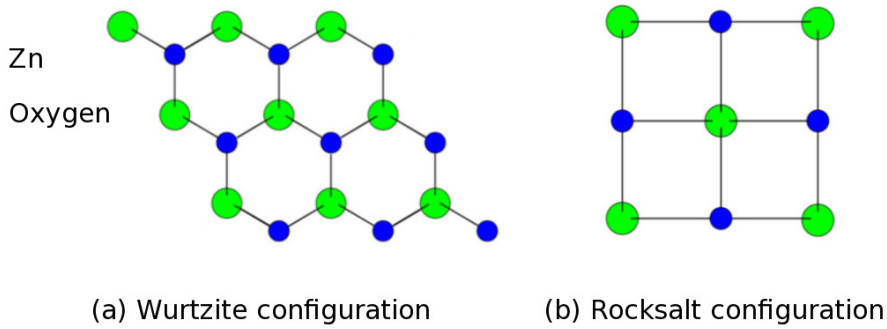

Figure 1. ZnO structure (ab-plane). (**a**) non-centrosymmetric, hexagonal, wurtzite configuration; (**b**) centrosymmetric, cubic, rocksalt configuration (Rochelle salt) [30–32]. The rocksalt configuration is distinguished by a tunable gap from 1.8 eV up to 6.1 eV, a gap value of 2.45 eV is typical for the monocrystal rocksalt configuration without oxygen vacancies [33,34]. As such, the rocksalt configuration could be suited for higher harmonics generation under non-equilibrium topological excitation [35,36].

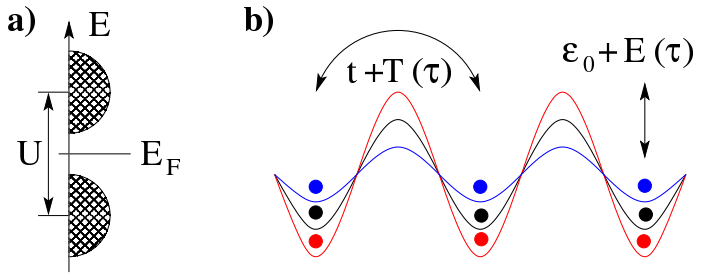

Figure 2. Insulator to metal transition caused by photo-excitation. (**a**) schematic split of energy bands due to the local Coulomb interaction U. The gap is determined symmetrically to the Fermi edge E_F; (**b**) the periodic in time driving yields an additional hopping contribution $T(\tau)$ of electrons on the lattice (black) and the renormalization of the local potential, $E(\tau)$, as a quasi-energy. Colors of the lattice potential represent the external driving in time.

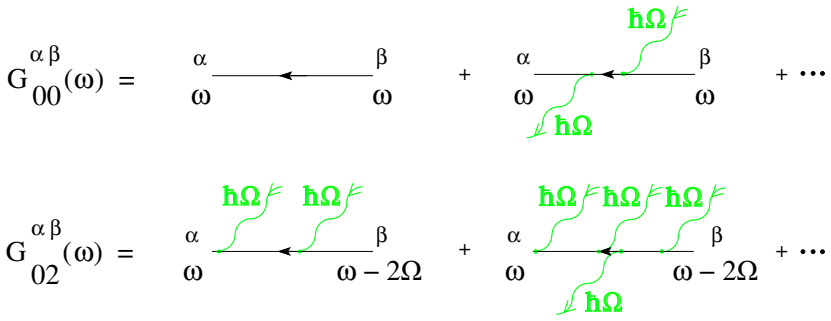

Figure 3. Schematic representation of the Floquet Green's function and the Floquet matrix in terms of absorption and emission of external energy quanta $\hbar\Omega$. $G_{00}^{\alpha\beta}(\omega)$ represents the sum of all balanced contributions; $G_{02}^{\alpha\beta}(\omega)$ describes the net absorption of two photons. α, β are the Keldysh indices.

2. Quantum Many Body Theory for Correlated Electrons in the Non-Equilibrium

We consider in this work the wide gap semiconductor bulk to be driven by a strong periodic-in-time external field in the optical range which yields higher-order photon absorption processes. The electronic dynamics of the photo-excitation processes, see Figure 2, is theoretically modelled by a generalized, driven, Hubbard Hamiltonian, see Equation (1). The system is solved with a Keldysh formalism including the electron-photon interaction in the sense of the coupling of the classical electromagnetic field to the electronic dipole and thus to the electronic hopping. This yields an additional kinetic contribution. We solve the system by the implementation of a dynamical mean field theory (DMFT), see Figure 4, with a generalized iterative perturbation theory solver (IPT), see Figure 5. The full interacting Hamiltonian, Equation (1), is introduced as follows:

$$\begin{aligned} H &= \sum_{i,\sigma} \varepsilon_i c_{i,\sigma}^{\dagger} c_{i,\sigma} + \frac{U}{2} \sum_{i,\sigma} c_{i,\sigma}^{\dagger} c_{i,\sigma} c_{i,-\sigma}^{\dagger} c_{i,-\sigma} \\ &\quad - t \sum_{\langle ij \rangle,\sigma} c_{i,\sigma}^{\dagger} c_{j,\sigma} \\ &\quad + i\vec{d} \cdot \vec{E}_0 \cos(\Omega_L \tau) \sum_{<ij>,\sigma} \left(c_{i,\sigma}^{\dagger} c_{j,\sigma} - c_{j,\sigma}^{\dagger} c_{i,\sigma} \right). \end{aligned} \tag{1}$$

In our notation, see Equation (1), $c^{\dagger}$, (c) are the creator (annihilator) of an electron. The subscripts i, j indicate the site, $\langle i, j \rangle$ implies the sum over nearest neighboring sites.

The term $\frac{U}{2} \sum_{i,\sigma} c_{i,\sigma}^{\dagger} c_{i,\sigma} c_{i,-\sigma}^{\dagger} c_{i,-\sigma}$ results from the repulsive onsite Coulomb interaction U between electrons with opposite spins. The third term $-t \sum_{\langle ij \rangle,\sigma} c_{i,\sigma}^{\dagger} c_{j,\sigma}$ describes the standard hopping processes of electrons with the amplitude t between nearest neighboring sites. Those contributions form the standard Hubbard model, which is generalized for our purposes in what follows. The first term $\sum_{i,\sigma} \varepsilon_i c_{i,\sigma}^{\dagger} c_{i,\sigma}$ generalizes the Hubbard model with respect to the onsite energy, see Figure 2. The electronic on-site energy is noted as ε_i. The external time-dependent electromagnetic driving is described in terms of the field $\vec{E}_0$ with laser frequency Ω_L, τ, which couples to the electronic dipole $\hat{d}$ with strength $|\mathbf{d}|$. The expression $i\vec{d} \cdot \vec{E}_0 \cos(\Omega_L \tau) \sum_{<ij>,\sigma} \left(c_{i,\sigma}^{\dagger} c_{j,\sigma} - c_{j,\sigma}^{\dagger} c_{i,\sigma} \right)$ describes the renormalization of the standard electronic hopping processes, as one possible contribution $T(\tau)$ in Figure 2, due to external influences.

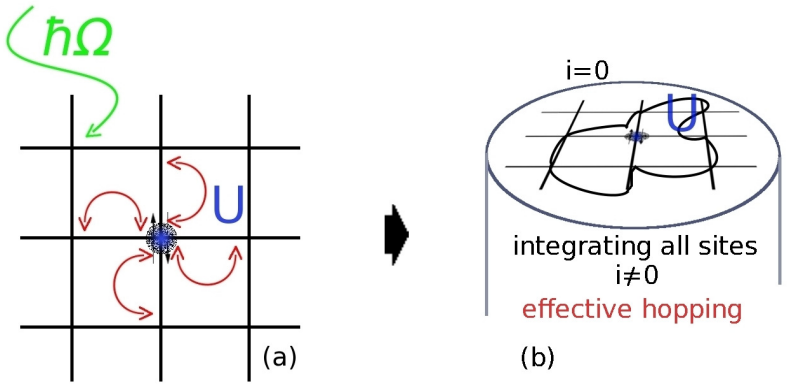

Figure 4. Schematic representation of non-equilibrium dynamical mean field theory. (**a**) the semiconductor behaves in the here considered regime as an insulator: Optical excitations by an external electromagnetic field with the energy $\hbar\Omega$ yield additional hopping processes. These processes are mapped onto the interaction with the single site on the background of the surrounding lattice bath in addition to the regular kinetic processes and in addition to on-site Coulomb repulsion; (**b**) DMFT idea: The integration over all lattice sites leads to an effective theory including non-equilibrium excitations. The bath consists of all single sites and the approach is thus self-consistent. The driven electronic system may in principal couple to a surface-resonance or an edge state. The coupling to these states can be enhanced by the external excitation.

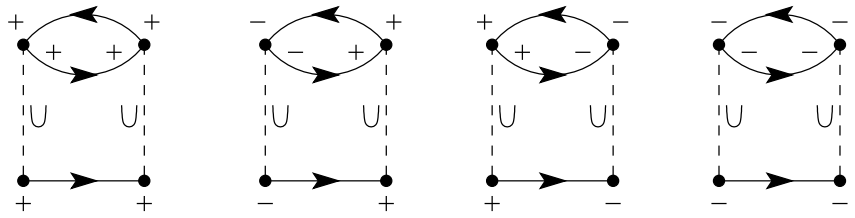

Figure 5. Local self-energy $\Sigma^{\alpha\beta}$ within the iterated perturbation theory (IPT). The IPT as a second order diagrammatic solver with respect to the electron electron interaction U is here generalized to non-equilibrium, $\pm$ indicates the branch of the Keldysh contour. The solid lines represent the bath in the sense of the Weiss-field $\mathcal{G}^{\alpha\beta}$; see Ref. [37].

2.1. Floquet States: Coupling of a Classical Driving Field to a Quantum Dynamical System

By introducing the explicit time dependency of the external field, we solve the generalized Hubbard Hamiltonian, see Equation (1). It yields Green's functions which depend on two separate time arguments which are Fourier transformed to frequency coordinates. These frequencies are chosen as the relative and the center-of-mass frequency [38,39] and we introduce an expansion into Floquet modes

$$\begin{aligned} G^{\alpha\beta}_{mn}(\omega) &= \int \mathrm{d}\tau_1^\alpha \mathrm{d}\tau_2^\beta \; e^{-i\Omega_L(m\tau_1^\alpha - n\tau_2^\beta)} e^{i\omega(\tau_1^\alpha - \tau_2^\beta)} G(\tau_1^\alpha, \tau_2^\beta) \\ &\equiv G^{\alpha\beta}(\omega - m\Omega_L, \omega - n\Omega_L). \end{aligned} \tag{2}$$

In general, Floquet [29] states are analogues to Bloch states. Whereas Bloch states are due to the periodicity of the potential in space, the spatial topology, the Floquet states represent the temporal topology in the sense of the temporal periodicity [35,38–46]. The Floquet expansion is introduced in Figure 3 as a direct graphic representation of what is described in Equation (2). The Floquet modes are labelled by the indices (m, n), whereas (α, β) refer to the branch of the Keldysh contour $(\pm)$ and the respective time argument. The physical consequence of the Floquet expansion, however, is noteworthy, since it can be understood as the quantized absorption and emission of energy $\hbar\Omega_L$ by the driven quantum many body system out of and into the classical external driving field.

In the case of uncorrelated electrons, $U = 0$, the Hamiltonian can be solved analytically and the retarded component of the Green's function $G_{mn}(k,\omega)$ reads

$$G^R_{mn}(k,\omega) = \sum_{\rho} \frac{J_{\rho-m}\left(A_0\tilde{\epsilon}_k\right) J_{\rho-n}\left(A_0\tilde{\epsilon}_k\right)}{\omega - \rho\Omega_L - \epsilon_k + i0^+}. \tag{3}$$

Here, $\tilde{\epsilon}_k$ is the dispersion relation induced by the external driving field. $\tilde{\epsilon}_k$ is to be distinguished from the lattice dispersion ϵ. J_n are the cylindrical Bessel functions of integer order, $A_0 = \vec{d}\cdot\vec{E}_0$, Ω_L is the external laser frequency. The retarded Green's function for the optically excited band electron is eventually given by

$$G^R_{\mathrm{Lb}}(k,\omega) = \sum_{m,n} G^R_{mn}(k,\omega). \tag{4}$$

2.2. Dynamical Mean Field Theory in the Non-Equilibrium

The generalized Hubbard model for the correlated system, $U \neq 0$, in the non-equilibrium, Equation (1), is numerically solved by a single-site Dynamical Mean Field Theory (DMFT) [37,46–59]. The expansion into Floquet modes with the proper Keldysh description models the external time dependent classical driving field, see Section 2.1, and couples it to the quantum many body system. We numerically solve the Floquet-Keldysh DMFT [37,46] with a second order iterative perturbation theory (IPT), where the the local self-energy $\Sigma^{\alpha\beta}$ is derived by four bubble diagrams; see Figure 5. The Green's function for the interaction of the laser with the band electron $G^R_{\mathrm{Lb}}(k,\omega)$, Equation (4), is characterized by the wave vector k, where k describes the periodicity of the lattice. It depends on the electronic frequency ω and the external driving frequency Ω_L, see Equation (2), captured in the Floquet indices (m,n). The DMFT self-consistency relation assumes the form of a matrix equation of non-equilibrium Green's functions, which is of dimension 2×2 in regular Keldysh space and of dimension $n\times n$ in Floquet space. The numerical algorithm is efficient and stable also for all values of the Coulomb interaction U.

In previous work [37,46,56], we considered an additional kinetic energy contribution due to a lattice vibration. Here, we take into account a coupling of the microscopic electronic dipole moment to an external electromagnetic field [38,39] for a correlated system. We introduce the quantum-mechanical expression for the electronic dipole operator $\hat{d}$, see the last term r.h.s. Equation (1), and this coupling reads as $i\vec{d}\cdot\vec{E}_0\cos(\Omega_L\tau)\sum_{<ij>,\sigma}\left(c^\dagger_{i,\sigma}c_{j,\sigma} - c^\dagger_{j,\sigma}c_{i,\sigma}\right)$. This kinetic contribution is conceptually different from the generic kinetic hopping of the third term of Equation (1). The coupling $\hat{d}\cdot\vec{E}_0\cos(\Omega_L\tau)$ generates a factor Ω_L that cancels the $1/\Omega_L$ in the renormalized cylindrical Bessel function in Equation (7) of Ref. [37] in the Coulomb gauge, $\vec{E}(\tau) = -\frac{\partial}{\partial\tau}\vec{A}(\tau)$ that is written in Fourier space as $\vec{E}(\Omega_L) = i\Omega_L\cdot\vec{A}(\Omega_L)$. The Floquet sum, which is a consistency check, is discussed in Section 3.3.

It has been shown by Ref. [49] that the coupling of an electromagnetic field modulation to the onsite electronic density $n_i = c^\dagger_{i,\sigma}c_{i,\sigma}$ in the unlimited three-dimensional translationally invariant system alone can be gauged away. This type of coupling can be absorbed in an overall shift of the local potential while no additional dispersion is reflecting any additional functional dynamics of the system. Therefore, such a system [26,60] will not show any topological effects as a topological insulator or a Chern insulator. In contrast, the coupling of the external electromagnetic field modulation to the dipole moment of the charges, and thus to the hopping term, see Equation (1), as a kinetic energy of the fermions, cannot be gauged away and is causing the development of topological states in the three-dimensional unlimited systems. A boundary as such is no necessary requirement. Line 3 of Equation (1) formally represents the electromagnetically induced kinetic contribution

$$i\vec{d}\cdot\vec{E}_0\cos(\Omega_L\tau)\sum_{<ij>,\sigma}\left(c^\dagger_{i,\sigma}c_{j,\sigma} - c^\dagger_{j,\sigma}c_{i,\sigma}\right) = e\sum_{\vec{r}}\hat{j}_{ind}(\vec{r})\cdot\vec{A}(\vec{r},\tau), \tag{5}$$

which is the kinetic contribution of the photo-induced charge current in-space dependent with $\vec{r}$

$$\vec{j}_{ind}(\vec{r})_{\delta} = -\frac{t}{i}\sum_{\sigma}(c^{\dagger}_{\vec{r},\sigma}c_{\vec{r}+\delta,\sigma} - c^{\dagger}_{\vec{r}+\delta,\sigma}c_{\vec{r},\sigma}). \tag{6}$$

The temporal modulation of the classical external electrical field in the (111) direction always causes a temporally modulated magnetic field contribution $\vec{B}(\vec{r},\tau) = \nabla \times \vec{A}(\vec{r},\tau)$ with $\vec{B}(\vec{r},\Omega_L)$ in Fourier space, as a consequence of Maxwell's equations. In the following, we derive the non-equilibrium local density of states (LDOS) which comes along with the dynamical life-time of non-equilibrium states as an inverse of the imaginary part of the self-energy $\tau \sim 1/\Im\Sigma^R$. A time reversal procedure induced by an external field will never be able to revise the non-equilibrium effect. The photon-electron coupling and thus the absorption will be modified and overall profoundly differing material characteristics are created. Conductivity and polarization of excited matter in the non-equilibrium are preventing any time-reversal processes in the sense of closing the Floquet fan again in this regime. The initial electromagnetic field thus causes a break of the time-reversal symmetry, and the current leads to the acquisition of a non-zero Berry flux. A Wannier-Stark type ladder [61] is created, which can be characterized by its Berry phase [62] as a Chern or a winding number or the $\mathbb{Z}_2$ invariants in three dimensions respectively [63].

3. Floquet Spectra of Driven Semiconductors

From the numerically computed components of the Green's function, we define [37] the local density of states (LDOS), $N(\omega,\Omega_L)$, where momentum is integrated out and Floquet indices are summed

$$N(\omega,\Omega_L) = -\frac{1}{\pi}\sum_{mn}\int \mathrm{d}^3k \mathrm{Im}\, G^R_{mn}(\mathbf{k},\omega,\Omega_L). \tag{7}$$

In combination with the lifetime as the inverse of the imaginary part of the self-energy, $\tau \sim 1/\Im\Sigma^R$, and the non-equilibrium distribution function

$$F^{neq}(\omega,\Omega_L) = \frac{1}{2}\left(1 + \frac{1}{2i}\frac{\sum_m G^{Keld}_{0m}(\omega,\Omega_L)}{\sum_n \mathrm{Im}G^A_{0n}(\omega,\Omega_L)}\right), \tag{8}$$

the local density of states $N(\omega,\Omega_L)$ can be experimentally determined as the compelling band structure of the non-equilibrium system.

We show results for optically excited semiconductor bulk, with a band gap in the equilibrium of 2.45 eV and typical parameters for ZnO. ZnO in either configuration [33,34,64–66] is a very promising material for the construction of micro-lasers, quantum wells and optical components. In certain geometries and in connection to other topological insulators, it is already used for the engineering of ultrafast switches. ZnO, see Figure 1, is broadly investigated in the non-centro-symmetric wurtzite configuration and very recently in the centro-symmetric rocksalt configuration [31,32]. Its bandgap is estimated to be of 1.8 eV up to 6.1 eV depending on various factors as the pressure during the fabrication process. In either crystal configuration, the production of second or higher order harmonics under intense external excitations [67] is searched. It is of high interest for novel types of lasers.

3.1. Development and Lifetimes of Floquet Topological Quantum States in the Non-Equilibrium

In Figure 6, we investigate a wide gap semi-conductor band structure, and the band gap in equilibrium is assumed to be 2.45 eV. The semiconductor bulk shall be exposed to an external periodic-in-time driving field. The system is so far considered as pure bulk, so we are investigating Floquet topological effects in the non-equilibrium without any other geometrical influence. The excitation intensity in the results of Figure 6a is considered to be 5.0 MW/cm^2 and 10.0 MW/cm^2 in Figure 6b. DMFT as a solver for correlated and strongly correlated electronics as such

is a spatially independent method. It is designed to derive bulk effects, whereas all k-dependencies have been integrated as the fundamental methodology. Therefore, we are not analyzing the k-resolved information of the Brillouin zone. As long as no artificial coarse graining with a novel length scale in the sense of finite elements or finite volumes is included, DMFT results in one, two and three dimensions are independent of any spatial information. In fact, however, the energy dependent LDOS profoundly changes with a varying excitation frequency and with a varying excitation intensity as well, which gives evidence that also the underlying k-dependent band structure is topologically modulated. A non-trivial topological structure of the Hilbert space is generated by external excitations even though our system in equilibrium is fully periodic in space and time. The time dependent external electrical field generates a temporally modulated magnetic field which results in a dynamical Wannier-Stark effect and the generation of Floquet states. Floquet states are the temporal analogue to Bloch states, and thus the argumentation by Zak [61] in principle applies for the generation of the Berry phase γ_m, since the solid is exposed to an externally modulated electromagnetic potential [62,68–70]. The Floquet quasi-energies, see Figure 3, are labeled by the Floquet modes in dependency to the external excitation frequency, and to the external excitation amplitude. The topological invariants, the Chern number as a sum over all occupied bands $n = \sum_{m=1}^{\nu} n_m \neq 0$ and the $\mathbb{Z}_2$ invariants include the Berry flux $n_m = 1/2\pi \int d^2\vec{k}(\nabla \times \gamma_m)$. The winding number is also consistently associated with the argument of collecting a non-zero Berry flux. We consider both regimes, where the driving frequency is smaller than the width of the semiconductor gap in equilibrium and also where it is larger and a very pronounced topology of states is generated. While the system is excited and thus evolving in non-equilibrium, a Berry phase is acquired and a non-zero Berry flux and thus a non-zero Chern number are characterizing the topological band structure as to be *non-trivial*. For one-dimensional, models [61,71] with the variation of the external excitation frequency Ω_L replica of Floquet bands with a quantized change of the Berry phase $\gamma = \pi$ emerge in the spectrum. In three dimensions, the Berry phase is associated with the Wyckoff positions of the crystal and the Brillouin zone [61], and, as such, it cannot be derived by the pure form of the DMFT. $\vec{k}$-dependent information can be derived by so-called real-space or cluster DMFT solutions (R-DMFT or CDMFT) [72–75]; however, they have not been generalized to the non-equilibrium for three-dimensional systems. It is important to note that the system out of equilibrium acquires a non-zero Berry phase and Coulomb interactions lead to a Mott-type gap that closes due to the superposition by crossing Floquet bands; however, the opening of non-equilibrium induced Mott-gap replica can also be found for $\Omega_L = 0.95$ eV. The replica are complete at $\Omega_L = 1.9$ eV; see Figure 6a. For the increase of $\vec{E}_0$, these gap replica are again intersected by the next order of Floquet sidebands. The closing of the Mott-gap and the opening of side Mott-gaps, in the spectrum due to topological excitation, are classified as *non-trivial* topological effects. In Figure 7a, we present results of the LDOS for the same system of optically excited cubic ZnO rocksalt excited by an external laser energy of 1.75 eV and an increasing excitation intensity, Figure 7b shows the corresponding inverse lifetime $\Im\Sigma^R$ and Figure 7c shows the corresponding non-equilibrium distribution of electrons F^{neq}. In addition, for very small excitation intensities, the result for the non-equilibrium distribution function F^{neq} shows a profound deviation from the Fermi step in equilibrium. These occupied non-equilibrium states have a finite lifetime, especially at the inner band edges, which is a sign of the Franz-Keldysh effect [76–79], here in the sense of a topological effect, which is accessible in a pump-probe experiment.

The change of the polarization of the external excitation modifies the physical situation and the result. In particular, circular and elliptically polarized light can be formally written as a superposition of linear polarized waves. Thus, in the pure uncorrelated case, $U = 0$, one could think that the setup can be formally implemented in the sense of coupled matrices. In the strongly correlated system at hand, the physics is fundamentally different. The solution for the strongly correlated case, $U \neq 0$, in the non-equilibrium, including DMFT, will become more sophisticated since the coupled matrices will result in the entanglement of processes in some sense. This can be deduced from the result in Figure 7b, which displays the modification of non-equilibrium life-times of electronic states due

to the varying excitation amplitudes. Such a modification is also qualitatively found for varying excitation frequencies.

The classification of correlated topological systems is an active research field [26,80,81]. At this point, we refer to Section 3.3 in this article, where we show, in our theoretical results the analysis of the single Floquet modes. For the investigation of the LDOS and the occupation number F^{neq}, as well as for the lifetimes of the non-equilibrium states, an artificial cut-off of the Floquet series, as it is described in the literature, does not make sense from the numerical physics point of view of DMFT in frequency space. This would hurt basically conservation laws and the cut-off would lead to a drift of the overall energy of the system; see Section 3.3. However, according to the bulk-boundary correspondence [2,3], the results of this work for bulk will be observed in a pump-probe experiment at the surface of the semiconductor sample. In the following, we discuss the development of Floquet topological states for an increasing external driving frequency Ω_L, see Figure 6, and, for an increasing amplitude of the driving, see Figure 7.

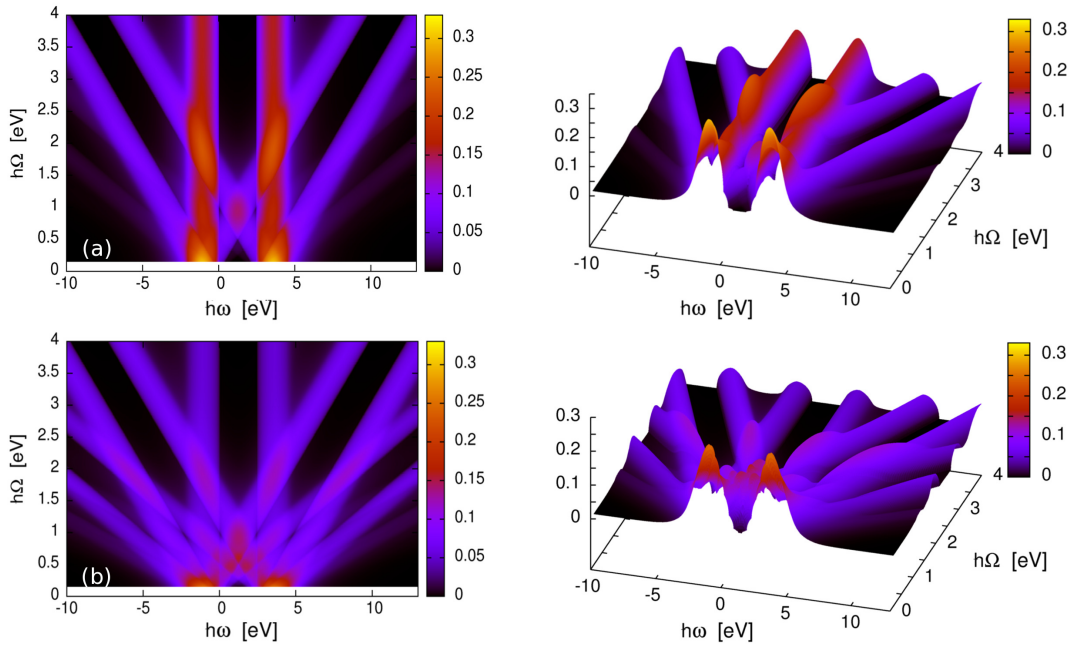

Figure 6. Floquet topological quantum states of the semiconductor bulk in the non-equilibrium. (**a**) the evolution of the LDOS in the non-equilibrium for varying excitation laser frequencies Ω_L up to $\Omega_L = 4.0$ eV is shown. The excitation intensity 5.0 MW/cm^2 is constant. The bandgap of ZnO rocksalt in equilibrium is 2.45 eV, see Figure 2, the gap is vanishing with the increase of the driving frequency and dressed states emerge as a consequence of the non-equilibrium AC-Stark effect [82,83]. The split bands are superposed by a doublet of Floquet fans which intersect. The formation of topological subgaps, see e.g., at $\hbar\Omega_L = 0.9$ eV occurs; (**b**) the evolution of the LDOS for the excitation intensity of 10.0 MW/cm^2 is shown. Spectral weight is shifted to a multitude of higher order Floquet-bands, while the original split band characteristics almost vanishes apart from the near-gap band edges. A variety of Floquet gaps is formed. At any crossing point, topologically induced transitions are possible, and the generation of higher harmonics can be enhanced. Panels on the right display the topology of the LDOS. The subgaps are very pronounced and the intersection of bands is visible as an increase of the LDOS which can be measurable in a pump-probe experiment. For a detailed discussion, please see Section 3.

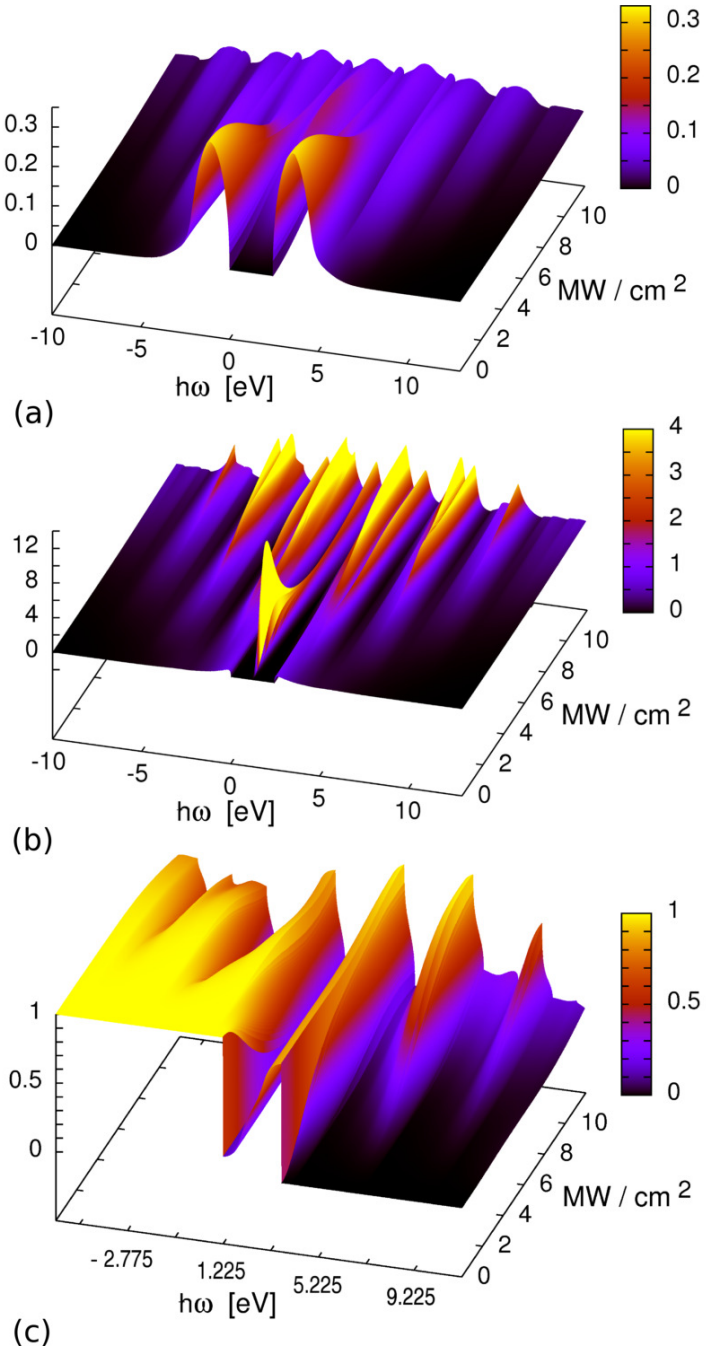

Figure 7. (**a**) energy spectra of Floquet topological quantum states of the semiconductor bulk in the non-equilibrium. The evolution of the LDOS is displayed for the single excitation energy of $\hbar\Omega_L = 1.75$ eV, wavelength $\lambda = 710.0$ nm and an increasing external driving intensity up to 10.0 MW/cm^2. Spectral weight is shifted by excitation to Floquet sidebands and a sophisticated sub gab structure is formed. In the non-equilibrium, such topological effects in correlated systems are non-trivial. The bandgap in equilibrium is 2.45 eV, the Fermi edge is 1.225 eV, and the width of each band is 2.45 eV as well; (**b**) inverse lifetime $\Im\Sigma^R$ of Floquet states of electromagnetically driven ZnO rocksalt bulk in the non-equilibrium; (**c**) non-equilibrium distribution function F^{neq} of electrons in optically driven bulk ZnO rocksalt. Parameters in (**b**,**c**) are identical to (**a**). For a detailed discussion, please see Section 3.

3.2. Topological Generation of Higher Harmonics and of Optical Transparency

When we increase the external excitation energy of the system Ω_L from 0 eV to 4.0 eV, Floquet topological quantum states as well as the topologically induced Floquet band gaps for bulk matter

are developed. Both valence and conduction band split in a multitude of Floquet sub-bands which cross each other. In Figure 6a, the evolution of a very clear Floquet fan for the valence as well as for the conduction band of the correlated matter in the non-equilibrium is found. When the excitation energy is increased up to 0.45 eV, the original band gap is subsequently closing, and the first crossing point in the semiconductor gap along the Fermi edge is found at 0.45 eV. With the increase of the excitation intensity, see Figure 6b, higher order Floquet sidebands are gaining spectral weight, and we find the next prominent crossing point at the Fermi edge for 0.2 eV. Band edges of higher order Floquet bands form crossing points with those of the first order. For an excitation energy of 0.42 eV, the crossing points of the first side bands (02) with the higher number side bands are found at the atomic energy of 1.08 eV and 2.3 eV, so above the valence band edge and deep in the gap of the semiconductor. Semiconductors are well known for fundamental absorption at the band edge of the valence band. We find here that the absorption coefficient of the semiconductor is topologically modulated. Non-trivial transitions at the crossing points of Floquet-valence subbands and Floquet-conduction subbands become significant. A higher order Floquet subband is usually physically reached by absorption or generation of higher harmonic procedures and we find a high probability for a topologically induced direct transitions from the fundamental to higher order bands for those points in the spectrum where a Floquet band edge intersects with the inner band edge of the equilibrium valence band. At any band edge directional scattering can be expected if the lifetimes of states are of a value that is applicable to the expected scattering processes. In general, the optical refractive index is topologically modulated, and electromagnetically induced transparency will become observable for intense excitations. The topologically induced Floquet bands overlap and cross each other. Consequentially, very pronounced features and narrow subgaps are formed in the LDOS, which correspond with sharp spikes in the expected life-times in the non-equilibrium. Floquet replica of valence and conduction bands are formed and the dispersion is renormalized. We also find regions for excitation energies from $\hbar\Omega_L = 0.5$ eV up to $\hbar\Omega_L = 0.85$ eV and from $\hbar\Omega_L = 1.1$ eV up to $\hbar\Omega_L = 1.45$ eV, which can be interpreted as a topologically induced metallic phase. These states are the result of the Franz-Keldysh effect [76–79] or AC-Stark effect, which is well known for high intensity excitation of semiconductor bulk and quantum wells [82,83].

From the viewpoint of correlated electronics in the non-equilibrium, we interpret our results as follows. For finite excitation frequencies, an instantaneous transition to the topologically induced Floquet band structure and a renormalized dispersion is derived. In the bulk system clear Floquet bands develop, if the sample is excited by an intense electrical field. This is observable in Figure 6.

In Figure 7, we display the same system as in Figure 6 for constant driving energy of 1.75 eV and an increasing driving intensity up to 10.0 MW/cm^2. We find the development of side bands and an overall vanishing semiconductor gap is found, which marks the transition from the semi-conductor to the topologically highly variable and switchable conductor in the non-equilibrium.

In this article, we do not investigate the coupling to a geometrical edge or a resonator mode. This will lead in the optical case to additional contributions in Equation (1) for the mode itself $\hbar\omega_o a^\dagger a$ and the coupling term of the resonator or edge mode to the electron system of the bulk $g\sum_{i,\sigma} c^\dagger_{i,\sigma} c_{i,\sigma}(a^\dagger + a)$. $a^\dagger$ and a are the creator and the annihilator of the photon, and g is the variable coupling strength of the photonic mode to the electronic system [84]. From our results, here we can conclude already that, for semi-conductor cavities and quantum wells as well as for structures which enhance so called edge states, these geometrical edge or surface resonances will induce an additional topological effect within the full so far excitonic spectrum. It is an additional effect that occurs beyond the bulk boundary correspondence. Dressed states may release energy quanta, e.g., light, or an electronic current into the resonator component [38]. Thus, we expect from our results that such modes may become a sensible switch in non-equilibrium.

It can be expected as well that novel topological effects in the non-equilibrium occur from the geometry. If the energy of the system is conserved, these modes will have always an influence on the full spectrum of the LDOS, when the system is otherwise periodic in space and time. Thus, it is

to clarify whether such modes may be of technological use. For the investigation of ZnO as a laser material, the influences of surface resonators will be subject to further investigations. It is on target to find out all the signatures of a topologically protected edge mode in correlated and strongly correlated systems out of equilibrium, and to classify the significance of topological effects for the occurrence of the electro-optical Kerr effect, the magneto-optical Kerr effect (MOKE) or the surface magneto-optical Kerr effect (SMOKE). We believe that in correlated many-body systems out of equilibrium a bulk boundary correspondence is given and will be experimentally found. Those results become modified or enhanced by a coupling of bulk states with the geometry of a micro- or a nanostructure and their geometrical resonances.

3.3. Consistency of the Numerical Framework

The consistency of the numerical formalism is generally checked by the sum over all Floquet indices with the physical meaning that energy conservation must be guaranteed in the non-equilibrium. Consequentially, we do not take into account thermalization procedures and the system's temperature remains constant. The analysis of the numerical validity as the normalized and frequency integrated density of states

$$N_i(\Omega_L) := \int \mathrm{d}\omega N(\omega, \Omega_L) = 1 \tag{9}$$

is confirmed in this work for summing over Floquet indices up to the order of 10. We discuss in Figure 8 on the l.h.s. the Floquet contributions with increasing number in steps of $n = 0, 2, 4, 6, 8, 10$. With an increasing order of the Floquet index, the amplitude of the Floquet contribution decreases towards the level of numerical precision of the DMFT self-consistency. This is definitely reached for $n = 10$ and thus it is the physical argument to cut the Floquet expansion off for $n = 10$. As a systems requirement, the Floquet contributions $G_{0\pm n}$ are perfectly mirror symmetric with respect to the Fermi edge, whereas the sum of both contributions is directly symmetric with respect to the Fermi edge. These symmetries are generally a proof of the validity of the numerical Fourier transformation and the numerical scheme. The order of magnitude of each Floquet contribution with a higher order than $n = 4$ is almost falling consistently with the rising Floquet index. We display results for the external laser wavelength of $\lambda = 710.0$ nm and the laser intensity of 3.8 MW/cm^2; the ZnO gap is assumed to be 2.45 eV, which is ZnO rocksalt as a laser active material. We include Floquet contributions up to a precision of 10^{-3} with regard to their effective difference from the final result on the r.h.s of Figure 8 as the sum to the nth-order. It corresponds to the accuracy of the self-consistent numerics.

The Floquet contributions, Figure 8, as such consequentially do not have a direct physical interpretation, however, the sum of all contributions is the local density of states, the LDOS, as a material characteristics. Whereas the lowest order Floquet contribution, compare Equation (2), G_{00} is symmetric to the Fermi edge but strictly positive, higher order contributions $G_{0\pm n}$ are mirror symmetric to each other and in sum they can have negative contributions to the result of the LDOS. The order of the Floquet contribution n numbers the evolving Floquet side bands which emerge in the LDOS, compare Figure 6a. The increase of mathematical and numerical precision has direct consequences for the finding and the accuracy of physical results, and the investigation of the coupling of the driven electronic system of the bulk with edge and surface modes will therefore profit. Bulk-surface coupling effects in nanostructure and waveguides are of great technological importance and the advantage of this numerical approach in contrast to time dependent DMFT frameworks in this respect is obvious.

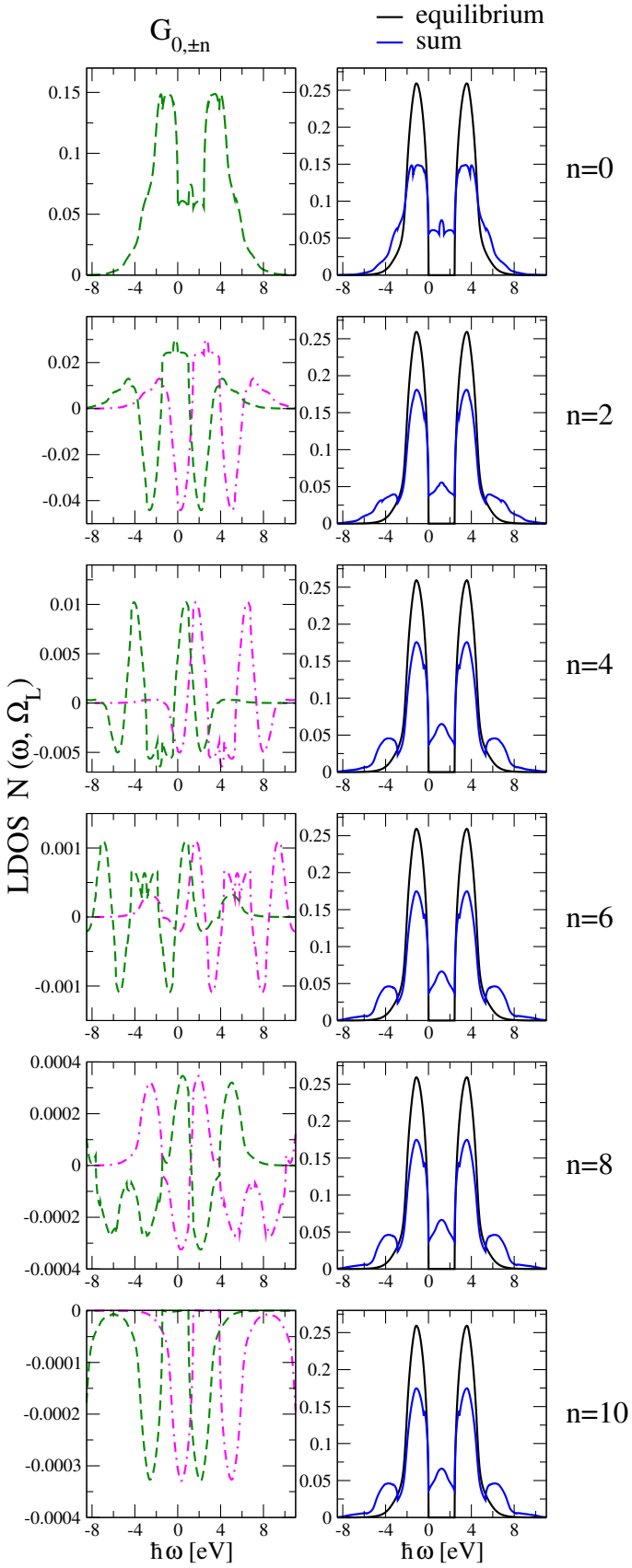

Figure 8. Floquet contributions and accuracy check of the numerical results for the LDOS of driven semiconductor bulk. The bandgap in equilibrium is 2.45 eV, the Fermi edge is 1.225 eV. For discussion, please see Section 3.3.

4. Conclusions

We investigated in this article the development of Floquet topological quantum states in wide band gap semiconductor bulk as a correlated electronic system with a generalized Hubbard model and with dynamical mean field theory in the non-equilibrium. We found that optical excitations induce a non-trivial band structure and, in several frequency ranges, a topologically induced metal phase is found as a result of the AC-Stark effect. The intersection of Floquet bands and band edges induces novel transitions, which may lead to up- and downconversion effects as well as to higher harmonic generation. The semiconductor absorption coefficient is topologically modulated. Non-trivial transitions at the crossing points of the underlying equilibrium band structure with the intersecting Floquet fans become possible and their efficiency is depending on the excitation power. We also find the development of pronounced novel sub gaps as areas of electromagnetically induced transparency. We also presented a consistency check as a physical consequence of the Floquet sum, which ensures numerically energy conservation. Our results for semiconductor bulk can be tested optoelectronic and magneto-optoelectronic experiments; they may serve as a guide towards innovative laser systems. The bulk semiconductor under topological non-equilibrium excitations as such has to be reclassified. It will be of great interest to investigate the interplay of topological bulk effects with additional surface resonances, a polariton coupling, or a surface magneto-optical modulation.

Author Contributions: Both authors equally contributed to the presented work. Both authors were equally involved in the preparation of the manuscript. Both authors have read and approved the final manuscript.

Funding: This research received no external funding.

Acknowledgments: The authors thank H. Monien, H. Wittel and F. Hasselbach for highly valuable discussions.

Conflicts of Interest: The authors declare that there are no conflict of interests.

References

1. Kosterlitz, J.M.; Thouless, D.J. Ordering, metastability and phase transitions in two-dimensional systems. *J. Phys. C Solid State Phys.* **1973**, *6*, 1181.
2. Fu, L.; Kane, C.L.; Mele, E.J. Topological Insulators in Three Dimensions. *Phys. Rev. Lett.* **2007**, *98*, 106803.
3. Hasan, M.Z.; Kane, C.L. Colloquium: Topological insulators. *Rev. Mod. Phys.* **2010**, *82*, 3045.
4. Fu, L.; Kane, C.L. Superconducting Proximity Effect and Majorana Fermions at the Surface of a Topological Insulator. *Phys. Rev. Lett.* **2008**, *100*, 096407.
5. Moore, G.; Read, N. Nonabelions in the fractional quantum hall effect. *Nucl. Phys. B* **1991**, *360*, 362.
6. Goldmann, N.; Dalibard, J. Periodically Driven Quantum Systems: Effective Hamiltonians and Engineered Gauge Fields. *Phys. Rev. X* **2014**, *4*, 031027.
7. Zutic, I.; Fabian, J.; Das Sarma, S. Spintronics: Fundamentals and applications. *Rev. Mod. Phys.* **2004**, *76*, 323.
8. Nayak, C.; Simon, S.H.; Stern, A.; Freedman, M.; Das Sarma, S. Non-Abelian anyons and topological quantum computation. *Rev. Mod. Phys.* **2008**, *80*, 1083.
9. Rechtsman, M.C.; Zeuner, J.M.; Plotnik, Y.; Lumer, Y.; Podolsky, D.; Dreisow, F.; Nolte, S.; Segev, M.; Szameit, A. Photonic Floquet topological insulators. *Nature* **2013**, *496*, 196.
10. Bandres, M.A.; Wittek, S.; Harari, G.; Parto, M.; Ren, J.; Segev, M.; Christodoulides, D.N.; Khajavikhan, M. Topological insulator laser: Experiments. *Science* **2018**, *359*, doi:10.1126/science.aar4005.
11. Lubatsch, A.; Frank R. A Self-Consistent Quantum Field Theory for Random Lasing. *Appl. Sci.* **2019**, *9*, 2477, doi:10.3390/app9122477.
12. Bernevig, B.A.; Hughes, T.L.; Zhang, S.-C. Quantum Spin Hall Effect and Topological Phase Transition in HgTe Quantum Wells. *Science* **2006**, *314*, 1757.
13. König, M.; Wiedmann, S.; Brüne, C.; Roth, A.; Buhmann, H.; Molenkamp, L.W.; Qi, X.-L.; Zhang, S.-C. Quantum spin hall insulator state in HgTe quantum wells. *Science* **2007**, *318*, 766.
14. Hsieh, D.; Qian, D.; Wray, L.; Xia, Y.; Hor, Y.S.; Cava, R.J.; Hasan, M.Z. A topological Dirac insulator in a quantum spin Hall phase : Experimental observation of first strong topological insulator. *Nature* **2008**, *452*, 970–974.

15. Xia, Y.; Qian, D.; Hsieh, D.; Wray, L.; Pal, A.; Lin, H.; Bansil, A.; Grauer, D.; Hor, Y.S.; Cava, R.J.; et al. Discovery (theoretical prediction and experimental observation) of a large-gap topological-insulator class with spin-polarized single-Dirac-cone on the surface. *Nat. Phys.* **2009**, *5*, 398.
16. Zhang, H.; Liu, C.-X.; Qi, X.-L.; Dai, X.; Fang, Z.; Zhang, S.-C. Topological insulators in Bi_2Se_3, Bi_2Te_3 and Sb_2Te_3 with a single Dirac cone on the surface. *Nat. Phys.* **2009**, *5*, 438–442.
17. Lindner, N.H.; Refael, G.; Galitski, V. Floquet Topological Insulator in Semiconductor Quantum Wells. *Nat. Phys.* **2011**, *7*, 490–495.
18. Katan, Y.T.; Podolsky, D. Modulated Floquet Topological Insulators. *Phys. Rev. Lett.* **2013**, *110*, 016802.
19. Rudner, M.S.; Lindner, N.H.; Berg, E.; Levin, M. Anomalous Edge States and the Bulk-Edge Correspondence for Periodically Driven Two-Dimensional Systems. *Phys. Rev. X* **2013**, *3*, 031005.
20. Wang, Y.; Liu, Y.; Wang, B. Effects of light on quantum phases and topological properties of two-dimensional Metal-organic frameworks. *Sci. Rep.* **2016**, *4*, 41644.
21. Kitagawa, T.; Oka, T.; Brataas, A.; Fu, L.; Demler, E. Transport properties of nonequilibrium systems under the application of light: Photoinduced quantum Hall insulators without Landau levels. *Phys. Rev. B* **2011**, *84*, 235108.
22. Gu, Z.; Fertig, H.A.; Arovas, D.P.; Auerbach, A. Floquet Spectrum and Transport through an Irradiated Graphene Ribbon. *Phys. Rev. Lett.* **2011**, *107*, 216601.
23. Wang, Y.H.; Steinberg, H.; Jarillo-Herrero, P.; Gedik N. Observation of Floquet-Bloch States on the Surface of a Topological Insulator. *Science* **2013**, *342*, 453–457.
24. Lindner, N.H.; Bergman, D.L.; Refael, G.; Galitski, V. Topological Floquet spectrum in three dimensions via a two-photon resonance. *Phys. Rev. B* **2013**, *87*, 235131.
25. Jiang, L.; Kitagawa, T.; Alicea, J.; Akhmerov, A.R.; Pekker, D.; Refael, G.; Cirac, J.I.; Demler, E.; Lukin, M.D.; Zoller, P. Majorana Fermions in Equilibrium and in Driven Cold-Atom Quantum Wires. *Phys. Rev. Lett.* **2011**, *106*, 220402.
26. D'Alessio, L. Rigol, Dynamical preparation of Floquet Chern insulators. *Nat. Commun.* **2015**, *6*, 8336.
27. Grushin, A.G.; Gomez-Leon, A.; Neupert, T. Floquet Fractional Chern Insulators. *Phys. Rev. Lett.* **2014**, *112*, 156801.
28. Bergholtz, E.; Liu, Z. Topological Flat Band Models and Fractional Chern Insulators. *Int. J. Mod. Phys. B* **2013**, *27*, 1330017.
29. Floquet, G. Sur les équations différentielles linéaires à coefficients périodiques. *Ann. l' Ecole Norm. Sup.* **1883**, *12*, 47–88.
30. Razavi-Khosroshahi, H.; Edalati, K.; Wu, J.; Nakashima, Y.; Arita, M.; Ikoma, Y.; Sadakiyo, M.; Inagaki, Y.; Staykov, A.; Yamauchi, M.; et al. High-pressure zinc oxide phase as visible-light-active photocatalyst with narrow band gap. *J. Mater. Chem. A* **2017**, *5*, 20298–20303.
31. Fritsch, D.; Schmidt, H.; Grundmann, M. Pseudopotential band structures of rocksalt MgO , ZnO , and Mg 1 x Zn x O. *Appl. Phys. Lett.* **2006**, *88*, 134104.
32. Dixit, H.; Saniz, R.; Lamoen, D.; Partoens, B. The quasiparticle band structure of zincblende and rocksalt ZnO. *J. Phys. Condens. Matter* **2010**, *22*, 125505.
33. Huang, F.; Lin, Z.; Lin, W.; Zhang, J.; Ding, K.; Wang, Y.; Zheng, Q.; Zhan, Z.; Yan, F.; Chen, D.; et al. Research progress in ZnO single-crystal: Growth, scientific understanding, and device applications. *Chin. Sci. Bull.* **2014**, *59*, 1235–1250.
34. Park, W.I.; Jun, Y.H.; Jung, S.W.; Yi, G.-C. Exciton emissions observed in ZnO single crystal nanorods. *Appl. Phys. Lett.* **2003**, *82*, 964–966.
35. Faisal, F.H.M.; Kaminski, J.Z. Floquet-Bloch theory of high-harmonic generation in periodic structures. *Phys. Rev. A* **1997**, *56*, 748.
36. Lubatsch, A.; Frank, R. Evolution of Floquet topological quantum states in driven semiconductors. *Eur. Phys. J. B* **2019**, *92*, 215, doi:10.1140/epjb/e2019-100087-0.
37. Frank, R. Quantum criticality and population trapping of fermions by non-equilibrium lattice modulations. *New J. Phys.* **2013**, *15*, 123030.
38. Frank, R. Coherent control of Floquet-mode dressed plasmon polaritons. *Phys. Rev. B* **2012**, *85*, 195463.
39. Frank, R. Non-equilibrium polaritonics - Nonlinear effects and optical switching. *Ann. Phys.* **2013**, *525*, 66–73.
40. Grifoni, M.; Hänggi, P. Driven quantum tunneling. *Phys. Rep.* **1998**, *304*, 229–354.

41. Restrepo, S.; Cerrillo, J.; Bastidas, V.M.; Angelakis, D.G.; Brandes, T. Driven Open Quantum Systems and Floquet Stroboscopic Dynamics. *Phys. Rev. Lett.* **2016**, *117*, 250401.
42. Eckardt, A. Colloquium: Atomic quantum gases in periodically driven optical lattices. *Rev. Mod. Phys.* **2017**, *89*, 011004-1.
43. Kalthoff, M.H.; Uhrig, G.S.; Freericks, J.K. Emergence of Floquet behavior for lattice fermions driven by light pulses. *Phys. Rev. B* **2018**, *98*, 035138.
44. Sentef, M.A.; Claassen, M.; Kemper, A.F.; Moritz, B.; Oka, T.; Freericks, J.K.; Devereaux, T.P. Theory of Floquet band formation and local pseudospin textures in pump-probe photoemission of graphene. *Nat. Commun.* **2015**, *6*, 7047.
45. Yuan, L.; Fan, S. Topologically non-trivial Floquet band structure in a system undergoing photonic transitions in the ultra-strong coupling regime. *Phys. Rev. A* **2015**, *92*, 053822.
46. Lubatsch, A.; Kroha, J. Optically driven Mott-Hubbard systems out of thermodynamical equilibrium. *Ann. Phys.* **2009**, *18*, 863–867.
47. Georges, A.; Kotliar, G.; Krauth, W.; Rozenberg, M.J. Dynamical mean-field theory of strongly correlated fermion systems and the limit of infinite dimensions. *Rev. Mod. Phys.* **1996**, *68*, 13.
48. Metzner, W.; Vollhardt, D. Correlated Lattice Fermions in $d = \infty$ Dimensions. *Phys. Rev. Lett.* **1989**, *62*, 324.
49. Schmidt, P.; Monien, H. Nonequilibrium dynamical mean-field theory of a strongly correlated system. *arXiv* **2002**, arXiv:0202046.
50. Maier, T.; Jarrell, M.; Pruschke, T.; Hettler, M.H. Quantum cluster theories. *Rev. Mod. Phys.* **2005**, *77*, 1027.
51. Freericks, J.K.; Turkowski, V.M.; Zlatic, V. Nonequilibrium Dynamical Mean-Field Theory. *Phys. Rev. Lett.* **2006**, *97*, 266408.
52. Tsuji, N.; Oka, T.; Aoki, H. Nonequilibrium Steady State of Photoexcited Correlated Electrons in the Presence of Dissipation. *Phys. Rev. Lett.* **2009**, *103*, 047403.
53. Lin, N.; Marianetti, C.A.; Millis, A.J.; Reichman, D.R. Dynamical Mean-Field Theory for Quantum Chemistry. *Phys. Rev. Lett.* **2011**, *106*, 096402.
54. Zgid, D.; Chan, G.K.-L. Dynamical mean-field theory from a quantum chemical perspective. *J. Chem. Phys.* **2011**, *134*, 094115.
55. Aoki, H.; Tsuji, N.; Eckstein, M.; Kollar, M.; Oka, T.; Werner, P. Nonequilibrium dynamical mean-field theory and its applications. *Rev. Mod. Phys.* **2014**, *86*, 779.
56. Frank, R. Population trapping and inversion in ultracold Fermi gases by excitation of the optical lattice-Non-equilibrium Floquet - Keldysh description. *Appl. Phys. B* **2013**, *113*, 41–47.
57. Sorantin, M.E.; Dorda, A.; Held, K.; Arrigoni, E. Impact ionization processes in the steady state of a driven Mott-insulating layer coupled to metallic leads. *Phys. Rev. B* **2018**, *97*, 115113.
58. Hofstetter, W.; Qin, T. Topological singularities and the general classification of Floquet-Bloch systems. *J. Phys. B At. Mol. Opt. Phys.* **2018**, *51*, 082001.
59. Qin, T.; Hofstetter, W. Nonequilibrium steady states and resonant tunneling in time-periodically driven systems with interactions. *Phys. Rev. B* **2018**, *97*, 125115.
60. Bukov, M.; D'Alessio, L.; Polkovnikov, A. Universal High-Frequency Behavior of Periodically Driven Systems: From Dynamical Stabilization to Floquet Engineering. *Adv. Phys.* **2015**, *64*, 139–226.
61. Zak, J. Berry's phase for energy bands in solids. *Phys. Rev. Lett.* **1989**, *62*, 2747–2750.
62. Xiao, D.; Chang, M.-C.; Niu, Q. Berry phase effects on electronic properties. *Rev. Mod. Phys.* **2009**, *82*, 1959–2007.
63. Gresch, D.; Autes, G.; Yazyev, O.V.; Troyer, M.; Vanderbilt, D.; Bernevig, B.A.; Soluyanov, A.A. Z2Pack: Numerical implementation of hybrid Wannier centers for identifying topological materials. *Phys. Rev. B* **2017**, *95*, 075146.
64. Chang, P.-C.; Lu, J.G. Temperature dependent conduction and UV induced metal-to-insulator transition in ZnO nanowires. *Appl. Phys. Lett.* **2008**, *92*, 212113.
65. Chang, P.-C.; Chien, C.-J.; Stichtenoth, D.; Ronning, C.; Lu, J.G. Finite size effect in ZnO nanowires. *Appl. Phys. Lett.* **2007**, *90*, 113101.
66. Koster, R.S.; Changming, M.F.; Dijkstra, M.; van Blaaderen, A.; van Huis, M.A. Stabilization of Rock Salt ZnO Nanocrystals by Low-Energy Surfaces and Mg Additions: A First-Principles Study. *J. Phys. Chem. C* **2015**, *119*, 5648–5656, doi: 10.1021/jp511503b.
67. Wegener, M. *Extreme Nonliner Optics*; Springer: Berlin/Heidelberg, Germany, 2004; ISBN 3-540-22291-X.

68. King-Smith, R.D.; Vanderbilt, D. Theory of polarization of crystalline solids. *Phys. Rev. B* **1993**, *47*, 1651–1654.
69. Vanderbilt, D.; King-Smith, R.D. Electric polarization as a bulk quantity and its relation to surface charge. *Phys. Rev. B* **1993**, *48*, 4442.
70. Resta, R. Macroscopic polarization in crystalline dielectrics: The geometric phase approach. *Rev. Mod. Phys.* **1994**, *66*, 899–915.
71. Dal Lago, V.; Atala, M.; Foa Torres, L.E.F. Floquet topological transitions in a driven one-dimensional topological insulator. *Phys. Rev. A* **2015**, *92*, 023624.
72. Gull, E.; Millis, A.; Lichtenstein, A.I.; Rubtsov, A.N.; Troyer, M.; Werner, P. Continuous-time Monte Carlo methods for quantum impurity models. *Rev. Mod. Phys.* **2011**, *83*, 349.
73. Snoek, M.; Titvinidze, I.; Toke, C.; Byczuk, K.; Hofstetter, W. Antiferromagnetic order of strongly interacting fermions in a trap: Real-space dynamical mean-field analysis. *New J. Phys.* **2008**, *10*, 093008.
74. Peters, R.; Yoshida, T.; Sakakibara, H.; Kawakami, N. Coexistence of light and heavy surface states in a topological multiband Kondo insulator. *Phys. Rev. B* **2016**, *93*, 235159.
75. Peters, R.; Yoshida, T.; Kawakami, N. Magnetic states in a three-dimensional topological Kondo insulator. *Phys. Rev. B* **2018**, *98*, 075104.
76. Franz, W. Einfluß eines elektrischen Feldes auf eine optische Absorptionskante. *Z. Naturforschung A* **1958**, *13*, 484–489.
77. Keldysh, L.V. The Effect of a Strong Electric Field on the Optical Properties of Insulating Crystals. Available online: jetp.ac.ru/cgi-bin/dn/e_007_05_0788.pdf (accessed on 4 October 2019).
78. Keldysh, L.V. Ionization in the Field of a Strong Electromagnetic Wave. Available online: jetp.ac.ru/cgi-bin/dn/e_020_05_1307.pdf (accessed on 4 October 2019).
79. Ivanov, A.L.; Keldysh, L.V. ; Panashchenko, V.V. Low-threshold exciton-biexciton optical Stark effect in direct-gap semiconductors. *Zh. Eksp. Teor. Fiz.* **1991**, *99*, 641–658.
80. Manmana, S.; Essin, A.M.; Noack, R.M.; Gurarie, V. Topological invariants and interacting one-dimensional fermionic systems. *Phys. Rev. B* **2012**, *86*, 205119.
81. Rachel, S. Interacting topological insulators: A review. *Rep. Prog. Phys.* **2018**, *81*, 116501.
82. Miller, D.A.B.; Chemla, D.S.; Damen, T.C.; Gossard, A.C.; Wiegmann, W.; Wood, T.H.; Burrus, C.A. Band-Edge Electroabsorption in Quantum Well Structures: The Quantum-Confined Stark Effect. *Phys. Rev. Lett.* **1984**, *53*, 2173–2176.
83. Chemla, D.S.; Knox, W.H.; Miller, D.A.B.; Schmitt-Rink, S.; Stark, J.B.; Zimmermann, R. The excitonic optical stark effect in semiconductor quantum wells probed with femtosecond optical pulses. *J. Lumin.* **1989**, *44*, 233–246.
84. Forn-Diaz, P.; Lamata, L.; Rico, E.; Kono, J.; Solano, E.; Ultrastrong coupling regimes of light-matter interaction. *Rev. Mod. Phys.* **2019**, *91*, 025005-1.